Superconducting nanowire single photon detectors based on disordered NbRe films

Cirillo, C.; Chang, J.; Caputo, M.; Los, J. W.N.; Dorenbos, S.; Esmaeil Zadeh, I.; Attanasio, C.

DOI
10.1063/5.0021487

Publication date
2020

Document Version
Final published version

Published in
Applied Physics Letters

Applied Physics Letters

Superconducting nanowire single photon detectors based on disordered NbRe films

Cite as: Appl. Phys. Lett. **117**, 172602 (2020); https://doi.org/10.1063/5.0021487
Submitted: 10 July 2020 . Accepted: 08 October 2020 . Published Online: 27 October 2020

C. Cirillo, J. Chang, M. Caputo, J. W. N. Los, S. Dorenbos, I. Esmaeil Zadeh, and C. Attanasio

Applied Physics Letters ARTICLE scitation.org/journal/apl

Superconducting nanowire single photon detectors based on disordered NbRe films

Cite as: Appl. Phys. Lett. **117**, 172602 (2020); doi: 10.1063/5.0021487
Submitted: 10 July 2020 · Accepted: 8 October 2020 ·
Published Online: 27 October 2020

C. Cirillo,[1,2,a] J. Chang,[3] M. Caputo,[2] J. W. N. Los,[4] S. Dorenbos,[4] I. Esmaeil Zadeh,[3] and C. Attanasio[1,2]

AFFILIATIONS

[1]CNR-SPIN, c/o Università degli Studi di Salerno, Via Giovanni Paolo II 132, 84084 Fisciano, SA, Italy
[2]Dipartimento di Fisica "E.R. Caianiello", Università degli Studi di Salerno, Via Giovanni Paolo II 132, 84084 Fisciano, SA, Italy
[3]Optics Research Group, ImPhys Department, Faculty of Applied Sciences, Delft University of Technology, Delft 2628 CJ, The Netherlands
[4]Single Quantum B.V., Delft 2628 CJ, The Netherlands

[a]Author to whom correspondence should be addressed: carla.cirillo@spin.cnr.it

ABSTRACT

Superconducting Nanowire Single Photon Detectors (SNSPDs) based on $Nb_{0.15}Re_{0.85}$ disordered nanowires are developed. The devices have a meander structure of wires 50–100 nm wide and cover a circular detection area with a diameter of about 10–16 μm. The main figures of merit of the detectors are extracted from a flood illumination process at 2.8 K, featuring a saturated internal efficiency up to $\lambda = 1301$ nm, recovery times between about 8 and 19 ns, and a jitter of about 35 ps. These results confirm that $Nb_{0.15}Re_{0.85}$ is a promising candidate for the realization of fast SNSPDs, as recently suggested.

Superconducting Single-Photon Detectors (SNSPDs)[1–3] are recognized as a mature platform for many applications such as, for instance, quantum information technology,[4] Light Detection And Ranging (LIDAR),[5] spectroscopy,[6] and mass spectrometry.[7] SNSPDs indeed fulfill the requirements of low dark count rates (DCRs),[8] high detection efficiency (DE),[9,10] fast response time,[11] and low timing jitter[12–14] in a rather wide spectral range.[15,16] Despite these high operation standards, great effort is constantly spent to both gain insight into the mechanism responsible for the detection process[17–19] and improve their performances. This last goal can be achieved by optimizing the properties of the materials-of-choice in this field,[20,21] by developing alternative device design,[1,22–24] and testing new superconductors.[1,25–27] As far as the choice of the material is concerned, a significant amount of work was recently devoted to the use of amorphous superconductors (for example, WSi, MoSi, and MoGe)[9,10,25] as alternatives to the traditionally employed NbN[28] and NbTiN.[12] Amorphous materials are distinguished for their detection performance in the mid-infrared region and for the robustness of their superconducting properties with respect to fabrication processing and surface roughness. However, as a consequence of their lower energy gap, they suffer from low time resolution, high dark counts, and low operation temperatures (<1 K).[1] It is clear that the figures of merit of the devices based on these two classes of materials (crystalline nitrides and amorphous superconductors) are deeply linked to their microscopic parameters.[1] Based on these considerations, NbRe films were recently proposed as valuable alternatives between typical crystalline nitride and amorphous films. One key parameter, which can be crucial for detecting lower energy photons (longer wavelength), is the value of the superconducting gap, Δ, that for NbRe is intermediate between the two kinds of materials. As a consequence, the detection can be extended to longer wavelengths with high efficiency (challenging with NbN, for instance) but working at temperatures accessible by cryogen-free technology (which is not the case for amorphous superconductors). Further advantages are represented by the reduced quasiparticle relaxation rates, almost an order of magnitude shorter than the ones of high-performing NbN wires, as well as larger expected hot-spot dimensions for the same incident photon energy.[29] The short relaxation rates are expected to produce short recovery times and good time resolution. On the other hand, with a large hot-spot radius, it is possible to design relatively wide nanowires and, consequently, reduce the problems of non-uniformities or constrictions along the devices. Moreover, as compared to NbN or other nitrides, the structural properties of NbRe films, made of small crystallites,[30] do not set strict requirements on the substrate or on the patterning procedures. Indeed, the superconducting properties are quite robust with respect to deposition and lithographic process, as well as to structural defects. NbRe films can be deposited on a variety of

TABLE I. Summary of the characteristics of the detectors under study.

Name	w (nm)	p (nm)	r (μm)	t_{rise} (ps)	t_{fall} (ns)	J_c (A/m^2)
D1	50	100	5	500	14.4	2.3×10^{10}
D2	60	120	5	425	8.15	2.0×10^{10}
D3	70	120	5	495	13.3	2.5×10^{10}
D4	70	140	8	700	18.8	2.0×10^{10}
D5	80	160	4.5	393	9.3	2.4×10^{10}
D6	80	160	4.5	425	7.43	3.2×10^{10}
D7	100	200	6	800	7.64	3.6×10^{10}

substrates and on large areas, which facilitates the optimization of the optical coupling and the absorption of the detectors. Finally, it is worth underlining that the films are grown by a single stoichiometric target in a pure Argon atmosphere, without requiring gas mixtures in the deposition chamber. This simplifies the sample deposition and assures good reproducibility. Here, the performances of nanowire single photon detectors with a meander design realized on 8-nm-thick NbRe films are reported and their main figures of merit are extracted. In particular, the dark count rate and internal detection efficiency at different wavelengths ($\lambda = 516$–1550 nm), the dead time, and the jitter were evaluated. In addition, variable angle ellipsometric measurements of the optical properties for $\lambda = 450$–1650 nm were performed. All the results are discussed and compared with the present literature.

NbRe films (composition $Nb_{0.15}Re_{0.85}$) were deposited by dc magnetron sputtering in a UHV system at room temperature on oxidized 2-in. Si wafers from a target with the same composition. The base pressure was $P \approx 8 \times 10^{-9}$ mbar, and the Ar pressure during the deposition was $P_{Ar} = 4 \times 10^{-3}$ mbar. The thickness of the NbRe film is $d_{NbRe} = 8$ nm, a value comparable with the superconducting coherence length estimated from upper critical field measurements, $\xi \sim 5$ nm.[30] At this reduced thickness, the films are expected to have a critical temperature, T_c, well above the liquid helium temperature, a normal state resistivity of about $\rho_n \approx 80\ \mu\Omega$·cm, and a residual resistivity ratio, $RRR \approx 0.7$, where RRR is the ratio between the resistance at room temperature, R_{RT}, and at $T = 10$ K, R_n.[30] The samples were patterned by Electron Beam Lithography (EBL) using a 100 KV e-beam (Raith EBPG-5200) on ARP-6200 (thickness ≈ 100 nm). The patterns were transferred to the NbRe layer by reactive ion etching with a SF_6/O_2 chemistry (12.5/3.4 standard cubic centimeter per minute). The resulting meanders were capped by 12 nm of SiN deposited by plasma enhanced chemical vapor deposition, to prevent the film oxidation. To evaluate the NbRe performance, a selection of the fabricated detectors was characterized and presented here. In the following results on several devices, differing in the nanowire linewidth, the pitch and covered area are reported. The devices' names and characteristics (linewidth w, pitch p, and radius r) are summarized in Table I. In Fig. 1(a), a scanning electron microscope (SEM) image of a photon detector meander with $w = 70$ nm and $p = 140$ nm is reported. The inset shows an enlarged image of the device, showing the well-defined nanowires. The devices were mounted on a flood illumination holder in a Gifford–McMahon closed cycle cryostat. All fabricated SNSPDs were superconducting, as a confirmation of the robust properties of the films that consist of small oriented crystallites.[30] In panel (b) of Fig. 1, the normalized resistive transition of the detector D3 is reported. The value of the critical temperature, defined at the midpoint of the transition curve, $T_c = 6.03$ K, is in agreement with published data on single unstructured films.[30] It is worth underlining that critical temperatures larger than 4.2 K simplify the complexity of the refrigeration system of a future NbRe-based detector.

Another important parameter along with T_c is the critical current, I_c. In earlier works, $V(I)$ characteristics were measured on micrometric strips either 15 or 5-nm-thick.[29,31] Here, the devices are characterized by voltage–current [$V(I)$] measurements at $T = 2.8$ K, as shown in panel (c) of Fig. 1 for all the analyzed detectors. The values of the corresponding critical current density for the different samples are reported in Table I. Here, it can be noticed that, despite the fact that devices D3, D4 and D5, D6 are nominally identical, they differ for the critical current density value, J_c. This can be ascribed to the fact that they were fabricated on pieces obtained from different locations on the wafer. It is useful to compare the results for J_c with the value of the depairing current density at the same reduced temperature, $t = T/T_c$, estimated according to the expression for $(J_{dp}(t)/J_{dp}(0))$ vs t obtained in the framework of the theory of Kupriyanov and Lukichev.[32] Since from Ref. 29, it is $J_{dp}(0) \approx 2 \times 10^{11}$ A/m^2, it follows that $J_{dp}(2.8\text{K}) \approx 5.5 \times 10^{10}$ A/m^2, a value comparable with the measured value of J_c, also considering the approximation used when estimating $J_{dp}(0)$. In principle, this result should assure a good detection

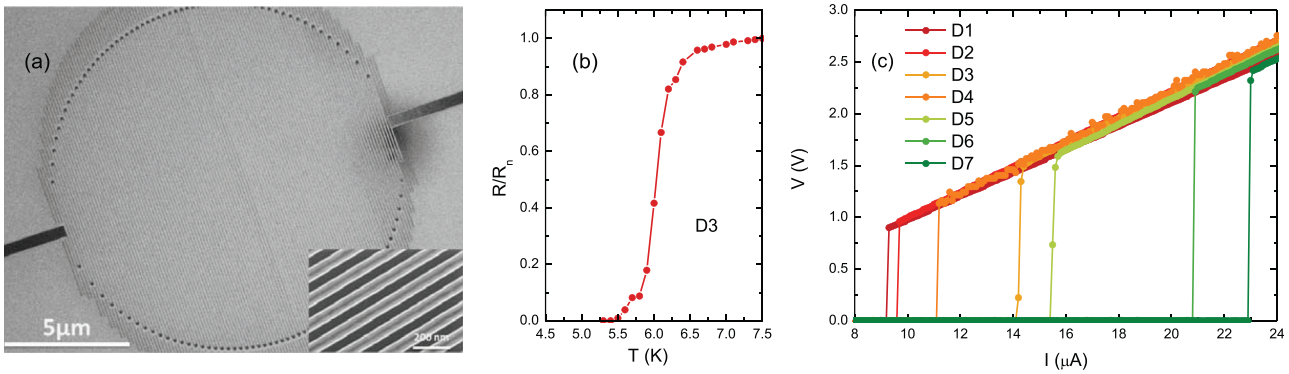

FIG. 1. (a) SEM image of typical fabricated devices with $w = 70$ nm and $p = 140$ nm. Inset: zoomed-in image of the detector. (b) Normalized resistive transition, R/R_n, of detector D3. (c) $V(I)$ characteristics measured at $T = 2.8$ K on the detectors reported in Table I.

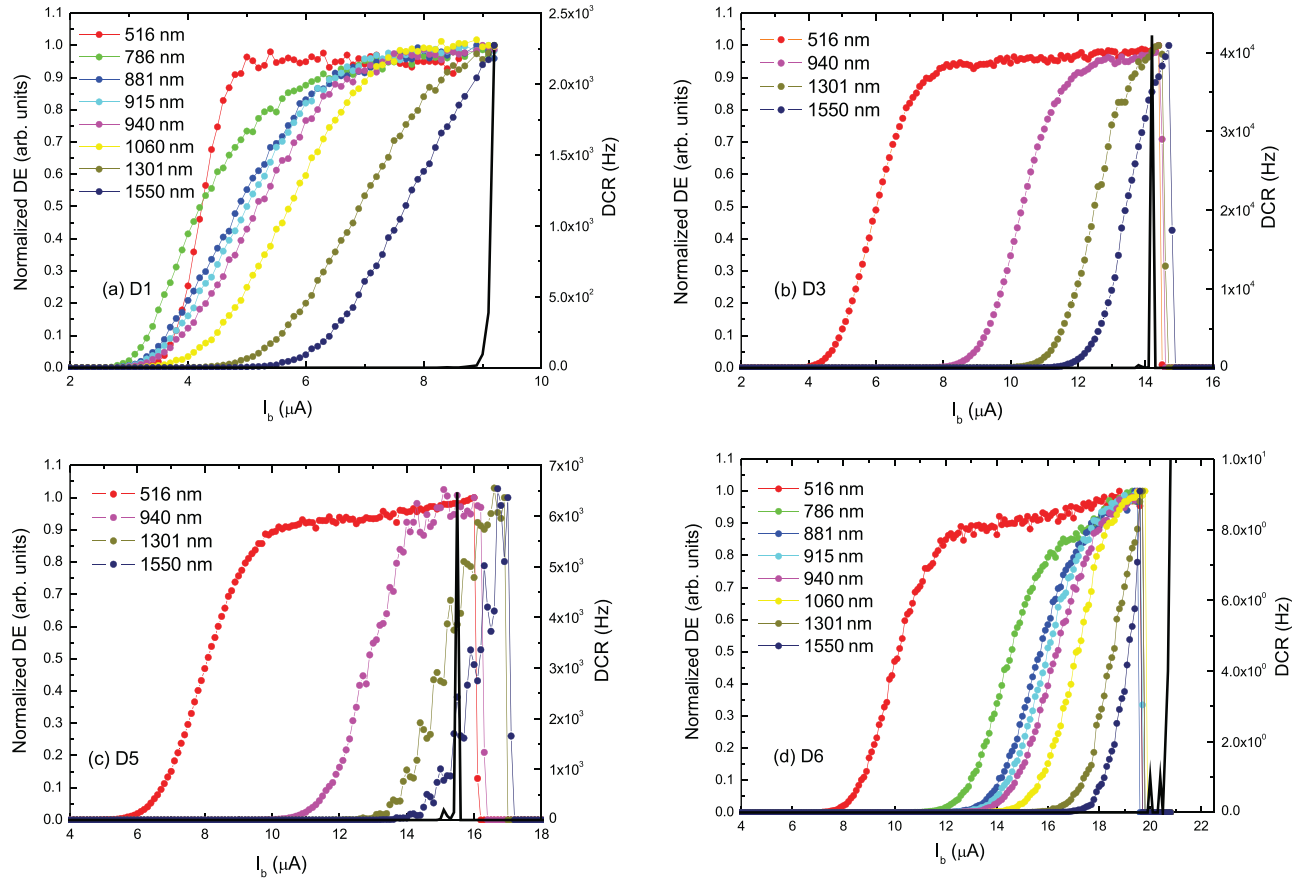

FIG. 2. Normalized detection efficiency (dark count rates) as a function of the bias current measured at different wavelengths at $T = 2.8$ K is reported on the left (right) scale. Each panel corresponds to a different NbRe-based detector.

efficiency.[1] As far as the DE is concerned, the literature suggests that the polycrystalline structure with small crystallites and disorder-dominated transport properties typical of NbRe films[29,30] should also promote high efficiency.[9] In order to gain insight into the detection performance of the NbRe-based devices, the internal efficiency as a function of the bias current, I_b, was measured by flood illumination at different wavelengths in the range of $\lambda = 516$–1550 nm, with the count rate of the devices kept around 100k events per second. The results, obtained at $T = 2.8$ K, are reported for a representative of samples in Fig. 2 (left scale), along with the dark count rate (right scale). The internal quantum efficiency significantly saturates at lower wavelengths for all the devices, but decreases at lower photon energy. Interestingly, for $\lambda = 516$–1060 nm, the saturation is reached for all the detectors at a value of I_b lower than the bias current at which the DCR starts to sensibly grow. These first results are encouraging since no optimizations of the film properties were implemented. The devices were also characterized in terms of time performance. In order to estimate the recovery time, the detectors were biased with a current I_b of about 95% of I_c and illuminated by a picosecond pulsed (5.2 ps) 1060 nm laser source. Single pulse and averaged pulses were recorded using a room temperature amplifier readout circuitry. Figure 3 presents the typical average voltage response as a function of time for

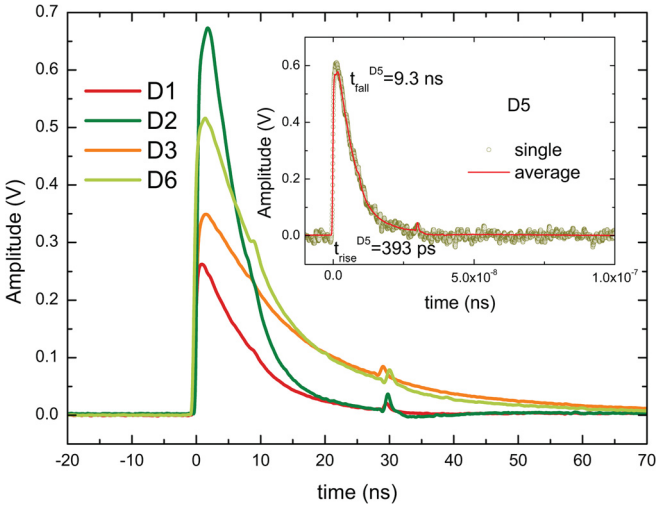

FIG. 3. Average waveform transient for a representative of NbRe-based detectors measured at $T = 2.8$ K. Inset: detection pulses for device D5 at $T = 2.8$ K; the single pulse data (points) are superimposed on the averaged measurement (line). The characteristic times, t_{rise}^{D5} and t_{fall}^{D5}, are indicated.

a selection of detectors, obtained from the average of 100 pulse traces from a 4 GHz bandwidth oscilloscope. In the inset, the average trace (line) is compared with a single shot pulse trace (points) for detector D5. Here, the characteristic times for the rise and fall sides, evaluated as the 20%–80% width of the rising edge and reduction of $1/e$ of the amplitude at the decaying side, respectively, are indicated. It results in the fact that the rise time spans from $t_{rise}^{D5} = 393$ ps of detector D5 to $t_{rise}^{D4} = 700$ ps and $t_{rise}^{D7} = 800$ ps of the wide area devices. The shortest fall time is $t_{fall}^{D5} = 9.3$ ns for detector D5, while t_{fall} is shorter than 20 ns for all the investigated devices. These values are competitive with those obtained for NbNTi-based SNSPD[12] and even superior to other high-performance amorphous materials investigated so far.[9,25,33] This result may be related to lower kinetic inductance compared to other platforms. The characteristic times of all the analyzed devices are summarized in Table I. Figure 4 shows the time jitter (points) measured on the detector D5 biased with a current of $I_b \approx 95\% \cdot I_c$ and illuminated by a 1030 nm ps pulsed laser. In order to enhance the signal to noise ratio, a cryogenic amplifier was used. The data are slightly asymmetric probably due to small resistance variations in different sections of the nanowire, which can be ascribed to the film oxidation.[14] The points can be fitted by a Gaussian dependence (see the line) and the timing jitter measurements evaluated as the full width half maximum (FWHM) equal to 35.1 ± 0.5 ps. This value is comparable with respect to NbNTi at $T = 4.3$ K,[15] but again much better than those for other amorphous materials.[9,34] Moreover, it can be further improved by tuning the film properties, as well as optimizing the detector design and fabrication.[1,12] Finally, NbRe optical absorption was evaluated by variable angle ellipsometry over the spectral range of $\lambda = 450$–1650 nm. Ellipsometric spectra were acquired at angles of incidence of 55°, 60°, 65°, and 70°. In order to estimate the complex refractive index, the data were fitted by using transfer matrix simulations of the absorption for TE polarization. The simulated structure comprises the following layers: air/NbRe(8 nm)/SiO_2(230 nm)/Au reflector(150 nm)/Si substrate. The results concerning the refractive index (n) and extinction (k) spectra as a function of λ are reported in Fig. 5. Both $n(\lambda)$ and $k(\lambda)$ present quite a steep increase at longer wavelengths. At $\lambda = 1550$ nm, $n = 6.22$ and $k = 5.90$. These values are higher than what were reported not only for films of MoSi, NbN, and NbTiN about 5-nm-thick but also for NbN films of 12 nm.[36] The inset of Fig. 5 shows the simulated absorption as a function of λ for different values of the devices' filling factor, $ff = w/p$. Interestingly, in the infrared range, the absorption is larger than 80% even for $ff = 0.2$, and at $\lambda = 1550$ nm, the highest absorption as large as 99.97% is obtained for moderate $ff = 0.4$. The last result, along with the large values estimated for k, suggests that it may be possible to realize devices with high absorption efficiency by using shorter meander with low ff, with the consequent effect of improving the time performance of the detector. The main figures of merit of the investigated devices confirm that NbRe is a promising material for the realization of SNSPD with high performances. The presented results are encouraging especially because this work represents a pilot study that was intended to probe the potentials of NbRe in the field of single photon detection. For these reasons, further investigation of detectors based on this promising material will be the subject of future works, with the aim of improving their performance. In particular, the efficiency can be enhanced by fine tuning the characteristic dimensions of the detector, for instance by reducing the thickness. Moreover, one could also test devices with micrometric wires, as suggested in recent works.[19,33] In addition, the deposition conditions may be systematically varied to match the optimal values of resistivity and critical temperature. In principle, a change in the film stoichiometry can also be explored since Nb_xRe_{1-x} compounds are all superconducting in the composition range of $0.13 \leq x \leq 0.38$, with a critical temperature varying from about 9 to 4 K, respectively.[35] Clearly, all the suggested investigations may be useful to improve the time performance of the devices. Moreover, it is desirable to perform further investigation to understand the detection mechanism involved in this material,[17,37] such as the study of vortex fluctuation and switching phenomena.[38,39] In conclusion, the promising performance of NbRe-based SNSPDs at an easily accessible cryogenic temperature was demonstrated. Due to both the reduced value of ξ and the disordered film structure,[30] the superconducting properties are robust with respect to the nanopatterning process. The devices show a clear saturated DE

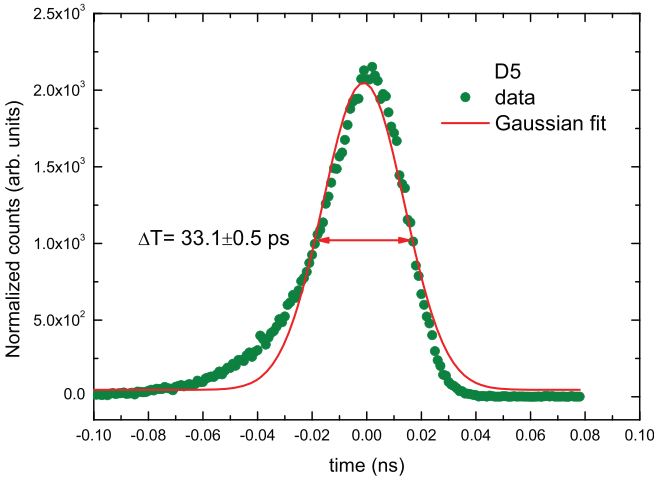

FIG. 4. Timing jitter for the detector D5 recorder at $T = 3.3$ K. See the text for details.

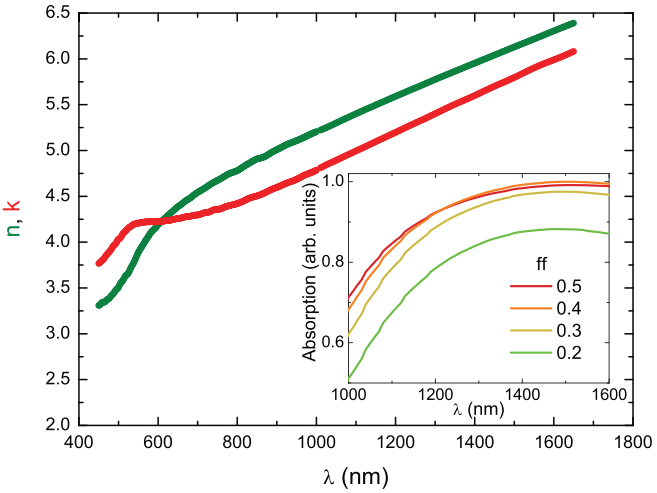

FIG. 5. Wavelength dependence of the refractive index (green line) and extinction coefficient (red line). Inset: wavelength dependence of the simulated absorption for different values of *ff*.

up to $\lambda = 1301$ nm at $T = 2.8$ K, with a time resolution, $\Delta T = 33.1$ ps. In addition, at infrared wavelengths, simulations return an extinction parameter exceeding 6, and an absorption of more than 99% for $ff = 0.4$, which may also indicate good performance of shorter devices. This work paves the way for the optimization of future devices based on NbRe, in particular, by tuning the film microscopical properties as well as geometry, along with the experimental setup, and NbRe-based devices may represent an alternative to nitride-based SNSPDs as well as to amorphous materials because of their improved performances in terms of time resolution and the operating temperature.

I. Esmaeil Zadeh acknowledges the High Tech Systems and Materials Research Program with Project No. 14660, financed by the Netherlands Organization for Scientific Research (NWO), Applied and Technical Sciences division (TTW) for funding this research. I. Esmaeil Zadeh acknowledges the support from the ATTRACT project funded by the EC under Grant Agreement No. 777222. J. Chang acknowledges the support from the China Scholarship Council (No. 201603170247).

DATA AVAILABILITY

The data that support the findings of this study are available from the corresponding author upon reasonable request.

REFERENCES

[1]I. Holzman and Y. Yachin, Adv. Quantum Technol. **2**, 1800058 (2019).
[2]C. M. Natarajan, M. G. Tanner, and R. H. Hadfield, Supercond. Sci. Technol. **25**, 063001 (2012).
[3]H. Zhang, L. Xiao, B. Luo, J. Guo, L. Zhang, and J. Xie, J. Phys. D **53**, 013001 (2020).
[4]H. Takesue, S. W. Nam, Q. Zhang, R. H. Hadfield, T. Honjo, K. Tamaki, and Y. Yamamoto, Nat. Photonics **1**, 343 (2007).
[5]A. McCarthy, N. J. Krichel, N. R. Gemmell, X. Ren, M. G. Tanner, S. N. Dorenbos, V. Zwiller, R. H. Hadfield, and G. S. Buller, Opt. Express **21**, 8904 (2013).
[6]R. Cheng, C.-L. Zou, X. Guo, S. Wang, X. Han, and H. X. Tang, Nat. Commun. **10**, 4104 (2019).
[7]N. Zen, A. Casaburi, S. Shiki, K. Suzuki, M. Ejrnaes, R. Cristiano, and M. Ohkubo, Appl. Phys. Lett. **95**, 172508 (2009).
[8]S. N. Dorenbos, E. M. Reiger, U. Perinetti, V. Zwiller, T. Zijlstra, and T. M. Klapwijk, Appl. Phys. Lett. **93**, 131101 (2008).
[9]F. Marsili, V. B. Verma, J. A. Stern, S. Harrington, A. E. Lita, T. Gerrits, I. Vayshenker, B. Baek, M. D. Shaw, R. P. Mirin, and S. W. Nam, Nat. Photonics **7**, 210 (2013).
[10]M. Caloz, M. Perrenoud, C. Autebert, B. Korzh, M. Weiss, C. Schönenberger, R. J. Warburton, H. Zbinden, and F. Bussiéres, Appl. Phys. Lett. **112**, 061103 (2018).
[11]A. Vetter, S. Ferrari, P. Rath, R. Alaee, O. Kahl, V. Kovalyuk, S. Diewald, G. N. Goltsman, A. Korneev, C. Rockstuhl, and W. H. P. Pernice, Nano Lett. **16**, 7085 (2016).
[12]I. Esmaeil Zadeh, J. W. N. Los, R. B. M. Gourgues, V. Steinmetz, G. Bulgarini, S. M. Dobrovolskiy, V. Zwiller, and S. N. Dorenbos, APL Photonics **2**, 111301 (2017).
[13]B. Korzh, Q.-Y. Zhao, J. P. Allmaras, S. Frasca, T. M. Autry, E. A. Bersin, A. D. Beyer, R. M. Briggs, B. Bumble, M. Colangelo *et al.*, Nat. Photonics **14**, 250 (2020).
[14]I. Esmaeil Zadeh, J. W. N. Los, R. B. M. Gourgues, J. Chang, A. W. Elshaari, J. R. Zichi, Y. J. van Staaden, J. P. E. Swens, N. Kalhor, A. Guardiani *et al.*, ACS Photonics **7**, 1780 (2020).
[15]R. B. M. Gourgues, J. W. N. Los, J. Zichi, J. Chang, N. Kalhor, G. Bulgarini, S. N. Dorenbos, V. Zwiller, and I. E. Zadeh, Opt. Express **27**, 24601 (2019).
[16]B. Baek, A. E. Lita, V. Verma, and S. W. Nam, Appl. Phys. Lett. **98**, 251105 (2011).
[17]A. Engel, J. J. Renema, K. Il'in, and A. Semenov, Supercond. Sci. Technol. **28**, 114003 (2015).
[18]J. J. Renema, R. Gaudio, Q. Wang, Z. Zhou, A. Gaggero, F. Mattioli, R. Leoni, D. Sahin, M. J. A. de Dood, A. Fiore, and M. P. van Exter, Phys. Rev. Lett. **112**, 117604 (2014).
[19]Y. Korneeva, N. Manova, I. Florya, M. Mikhailov, O. V. Dobrovolskiy, A. A. Korneev, and D. Yu. Vodolazov, Phys. Rev. Appl. **13**, 024011 (2020).
[20]J. Zichi, J. Chang, S. Steinhauer, K. V. Fieandt, J. W. N. Los, G. Visser, N. Kalhor, T. Lettner, A. W. Elshaari, I. Esmaeil Zadeh, and V. Zwiller, Opt. Express **27**, 26579 (2019).
[21]W. Zhang, Q. Jia, L. You, X. Ou, H. Huang, L. Zhang, H. Li, Z. Wang, and X. Xie, Phys. Rev. Appl. **12**, 044040 (2019).
[22]V. B. Verma, A. E. Lita, M. J. Stevens, R. P. Mirin, and S. W. Nam, Appl. Phys. Lett. **108**, 131108 (2016).
[23]S. Doerner, A. Kuzmin, S. Wuensch, I. Charaev, F. Boes, T. Zwick, and M. Siegel, Appl. Phys. Lett. **111**, 032603 (2017).
[24]F. Najafi, F. Marsili, V. B. Verma, Q. Zhao, M. D. Shaw, K. K. Berggren, and S. W. Nam, "Superconducting devices in quantum optics," in *Quantum Science and Technology*, edited by R. Hadfield and G. Johansson (Springer, Cham, 2016).
[25]V. B. Verma, A. E. Lita, M. R. Vissers, F. Marsili, D. P. Pappas, R. P. Mirin, and S. W. Nam, Appl. Phys. Lett. **105**, 022602 (2014).
[26]R. Arpaia, M. Ejrnaes, L. Parlato, F. Tafuri, R. Cristiano, D. Golubev, R. Sobolewski, T. Bauch, F. Lombardi, and G. P. Pepe, Physica C **509**, 16 (2015).
[27]O. V. Dobrovolskiy, D. Y. Vodolazov, F. Porrati, R. Sachser, V. M. Bevz, M. Yu. Mikhailov, A. V. Chumak, and M. Huth, Nat. Commun. **11**, 3291 (2020).
[28]C. Zhang, W. Zhang, J. Huang, L. You, H. Li, C. Iv, T. Sugihara, M. Watanabe, H. Zhou, Z. Wang, and X. Xie, AIP Adv. **9**, 075214 (2019).
[29]M. Caputo, C. Cirillo, and C. Attanasio, Appl. Phys. Lett. **111**, 192601 (2017).
[30]C. Cirillo, G. Carapella, M. Salvato, R. Arpaia, M. Caputo, and C. Attanasio, Phys. Rev. B **94**, 104512 (2016).
[31]C. Cirillo, M. Caputo, L. Parlato, M. Ejrnaes, D. Salvoni, R. Cristiano, G. P. Pepe, and C. Attanasio, Low Temp. Phys. **46**, 457 (2020).
[32]M. Y. Kupriyanov and V. F. Lukichev, Sov. J. Low Temp. Phys. **6**, 210 (1980).
[33]J. Chiles, S. M. Buckley, A. Lita, V. Verma, J. Allmaras, B. Korzh, M. D. Shaw, J. M. Shainline, R. P. Mirin, and S. W. Nam, Appl. Phys. Lett. **116**, 242602 (2020).
[34]V. B. Verma, B. Korzh, F. Bussiéres, R. D. Horansky, A. E. Lita, F. Marsili, M. D. Shaw, H. Zbinden, R. P. Mirin, and S. W. Nam, Appl. Phys. Lett. **105**, 122601 (2014).
[35]J. Chen, L. Jiao, J. L. Zhang, Y. Chen, L. Yang, M. Nicklas, F. Steglich, and H. Q. Yuan, Phys. Rev. B **88**, 144510 (2013).
[36]A. Banerjee, R. M. Heath, D. Morozov, D. Hemakumara, U. Nasti, I. Thayne, and R. H. Hadfield, Opt. Mater. Express **8**, 2072 (2018).
[37]D. Yu. Vodolazov, Phys. Rev. Appl. **7**, 034014 (2017).
[38]U. Nasti, L. Parlato, M. Ejrnaes, R. Cristiano, T. Taino, H. Myoren, R. Sobolewski, and G. P. Pepe, Phys. Rev. B **92**, 014501 (2015).
[39]A. Murphy, A. Semenov, A. Korneev, Y. Korneeva, G. Gol'tsman, and A. Bezryadin, Sci. Rep. **5**, 10174 (2015).